Desalination and Water Treatment
www.deswater.com

doi:10.5004/dwt.2016.0096

66 (2017) 299–308
March

Sonocatalytic degradation of organic pollutants by CdS nanoparticles hydrothermally prepared from cadmium(II) diethanoldithiocarbamate

Saeed Farhadi*, Firouzeh Siadatnasab

Department of Chemistry, Lorestan University, Khoramabad 68135-465, Iran, Tel. +98-66-33120611, Fax +98-66-33120618, email: sfarhadi1348@yahoo.com (S. Farhadi), n.siadatnasab@gmail.com (N. Siadatnasab)

Received 24 January 2016; Accepted 2 July 2016

ABSTRACT

In this work, CdS nanoparticles were prepared by hydrothermal decomposition of cadmium(II) diethanoldithiocarbamate ($Cd(DEDTC)_2$) precursor at 200°C and were used as a novel sonocatalyst for H_2O_2-assisted degradation of three organic dye pollutants including methylene blue (MB), Rhodamine B (RhB) and methyl orange (MO). This sonocatalyst was characterized using FT-IR, XRD, SEM, UV-Vis and EDX analysis which all of them confirmed the formation of high pure CdS nanoparticles with an average particle size of 20 nm. The optical absorption spectrum of CdS nanoparticles showed the band gap of 2.3 eV suitable for sonophotocatalytic degradation of organic pollutants. Under the optimized conditions, about 93% of RhB, 87% of MB and 55% of MO were degraded with the rate constants of 0.019, 0.014, and 0.0 04 min^{-1}, respectively. It was demonstrated that the sonocatalytic activity of CdS/ultrasound system was depended on CdS dosage, H_2O_2 concentration and initial dye concentration**.** The trapping experiments indicated that ·OH radicals were the main reactive species for dye degradation. In addition, the catalyst can be reused without significant loss of activity and its structure was not affected by the reactants or ultrasound.

Keywords: CdS nanoparticles; Hydrothermal synthesis; Sonocatalytic activity; Hydroxyl radical; Dyes degradation

1. Introduction

Nowadays, water pollution is a serious worldwide problem resulting in serious adverse impacts on the public health and environment. So, because of dyestuff industry propagation, wastewater of printing dye is one of the most considerable water pollution sources. It is estimated that around 10–15% of organic dyes mainly from industries are immoderately discharged into the rivers [1–3]. Various methods including biological processes, electrochemical process, membrane technology, adsorption, chemical oxidation and advanced oxidation processes (AOPs) have been developed to remove the dyes from polluted water concerning their low cost, simplicity of design, ease of operation and smaller amounts of harmful substances [4–12]. However, most of current degradation strategies still undesirably involve in several problems, such as low stability of catalyst, non-recyclability or complex operations for recycling. Therefore, finding better approaches to treat such dyes is rather imperative and significant.

The use of ultrasound waves as an advanced oxidation process has gained more attention for purification of polluted effluents because of its high efficiency and easy operation [13–16]. Rapid growth of the bubbles and their collapsing within the solution under ultrasound waves produce extremely high temperature and pressure leading to thermal dissociation of water and generation of hydroxyl radicals (·OH) as one of the most powerful non-selective oxidants for oxidation of target organic pollutants [13,17]. However, the application of ultrasound alone is not efficient for the degradation of the target organic pollutants because of the fact that the ultrasound alone requires more time and high amount of energy for an acceptable degradation. To overcome this problem, the active catalysts under ultrasonic irradiation (sonocatalysts), can be used for degrading organic pollutants in the aqueous phase. In the presence of an insoluble sonocatalyst, the generation of ·OH will be

*Corresponding author.

1944-3994 / 1944-3986 © 2017 Desalination Publications. All rights reserved.

accelerated during the ultrasonic irradiation [18,19]. In this context, using some metal oxide nanostructures such as Fe_3O_4, ZnO, and MgO were studied as sonocatalyst for degradation of organic dyes [20–23]. However, there is a need to develop new catalysts with high sonocatalytic activities.

In recent years, cadmium sulfide (CdS) with different nanostructures has been used as a photocatalyst for degradation of organic dye pollutants under different conditions [24–29]. However, there are several inherent drawbacks for CdS-based photocatalysts such as tendency of the CdS particles to aggregate and form larger particles, which results in surface area reduction and high recombination rate of photoinduced electron–hole pairs. Moreover, CdS involves in photocorrosion in aqueous media containing oxygen under light irradiation leading to its instability as a photocatalyst and its great practical application obstruction. On the other hand, the dye wastewater is usually non-transparent and highly-concentrated resulting in the light penetration limitation to only several millimeters. Therefore, there are some difficulties to degrade non-transparent and highly-concentrated dye wastewater via photocatalysis. As a solution, CdS sonocatalysis could be an appropriate candidate to overcome the above mentioned problems.

In this paper, we report the application of CdS nanoparticles as a novel sonocatalyst for degradation of MB, RB and MO in the aqueous solutions in the presence of H_2O_2 as a hydroxyl radical (·OH) source. The CdS nanoparticles were produced using hydrothermal decomposition of an air-stable, easily obtained single-source molecular precursor, namely cadmium(II) diethanoldithiocarbamate (Cd(DEDTC)$_2$) and characterized by X-ray diffraction (XRD), Fourier transform infrared spectroscopy (FT-IR), scanning electron microscopy (SEM), transmission electron microscope (TEM), energy dispersive X-ray (EDX) spectroscopy, and UV-visible spectroscopy. Also, the effect of some parameters such as amount of H_2O_2, sonocatalyst dosage and initial dye concentration was evaluated on the activity of CdS nanoparticles. To the best of the authors' knowledge and based on the literature review, there is no report on the use of CdS nanoparticles for the sonodegradation of organic dyes, especially in the presence of H_2O_2 as an environmental-friendly oxidizing agent.

2. Experimental

2.1. Materials

Diethanolamine ($C_4H_{11}NO_2$, 98%), cadmium nitrate ($Cd(NO_3)_2.4H_2O$, 99%), hydrogen peroxide (H_2O_2, 30%) and carbon disulfide (CS_2, 98%) were from Sigma-Aldrich. Methyl orange (MO, $C_{14}H_{14}N_3NaO_3S$), methylene blue (MB, $C_{16}H_{18}ClN_3S$) and Rhodamine B (RhB, $C_{28}H_{31}ClN_2O_3$) with high purity were from Merck chemical company.

2.2. Preparation of the Cd (DEDTC)$_2$ precursor complex

Initially, the Cd(DEDTC)$_2$ precursor complex was synthesized as follows: Diethanoldithiocarbamic acid was obtained from 0.02 mol (1.2 mL) of carbon disulfide and 0.02 mol (2 mL) of diethanolamine in 20 mL of 99.9% ethanol under ice cold condition (5°C). 20 mL of aqueous solution of $Cd(NO_3)_2{\cdot}4H_2O$ (3.08 g, 0.01 mol) was added to the yellow dithiocarbamic acid solution under continuous stirring and the final solution stirred for 30 min. Obtained Cd(DEDTC)$_2$ was filtered, washed with 40 mL of alcohol and then dried in an oven for 6 h at 60°C. Yield: 80%. Anal. Calc. for $CdC_{10}H_{20}N_2O_4S_4$: C, 25.4; H, 4.3; N, 6.1%. Found: C, 25.2; H, 4.0; N, 5.8%. Characteristic FT-IR data (KBr, cm^{-1}): 1480 ν(C-N) and 991 ν(C-S).

2.3. Preparation of CdS nanoparticles

For synthesizing the CdS nanoparticles, 0.5 g of the above prepared Cd(DEDTC)$_2$ precursor in 30 ml of distilled water was placed into a 50 mL Teflon-lined stainless steel autoclave and heated at 200°C for 24 h. The as-formed yellowish precipitate was filtered after cooling down to room temperature and washed with 20 mL of distilled water and ethanol 1:1 (v/v) mixture for three times, separately. The obtained CdS product was characterized with XRD, FT-IR, SEM, EDX, TEM and UV-visible spectroscopy.

2.4. Characterization techniques

The XRD patterns were inscribed on a Rigaku D-max C III, X-ray diffractometer using Ni-filtered Cu Ka radiation (k = 1.5406 Å) for decomposed samples phases determination. Infrared spectra were obtained using Schimadzu FT-IR 160 spectrophotometer using KBr pellets. The morphology of CdS nanoparticles was studied by Mira3 Tescan, scanning electron microscope outfitted with energy dispersive X-ray analyzer (EDX) for elemental analysis of the sample. The size of nanoparticles was determined by a transmission electron microscope (TEM, EM10C) at an accelerating voltage of 100 kV. Optical absorption spectra of nanocatalyst and dyes were obtained from a Cary 100 varian UV–Vis spectrophotometer in a wavelength range of 200–800 nm. Homogeneous suspension of nanocatalyst in ethanol for UV-Vis studies was formed by sonicating for 25 min. An ultrasonic apparatus operating at 37 kHz (Sonic 6MX, output acoustic power 100 W) was used for degradation of dye solutions. The concentration of Cd in the filtrate was determined by inductively coupled plasma atomic emission spectroscopy (ICP-AES, model OEC-730).

2.5. Sonocatalytic tests

Sonocatalytic activity of the CdS nanoparticles was evaluated by degradation of MB, RhB and MO in aqueous solutions under ultrasonic at room temperature. The reactions were conducted in a 100 mL Pyrex cylindrical glass vessel. In a typical experiment, the CdS nanoparticles (25 mg) were added to the dye solution (50 mL, 25 mg/L). Prior to ultrasonic irradiation, the mixtures were stirred for 30 min to achieve adsorption–desorption balance between the dye and sonocatalyst. The experiments were then performed under ultrasonic irradiation in the presence of H_2O_2 (1 M, 1.5 mL) in a dark place to avoid photoexcitation of CdS nanoparticles. At appropriate times, 2 mL of the dye solution was separated and centrifuged (5000 rpm, 10 min) to remove the catalyst. A UV-Vis spectrophotometer was used for analyzing the obtained clean transparent solu-

tion. The concentrations of MB, RhB and MO in the solutions were determined by UV-visible spectroscopy at 663, 557 and 462 nm, respectively. The degradation efficiency (%) of dyes was calculated using the following equation (Eq. (1)):

$$\text{Degradation efficiency } (\%) = \left[(C_0 - C)/C_0\right] \times 100 \quad (1)$$

where C_0 is the initial concentration of dye and C is the concentration of dye after reaction in specified exposure time. The effect of various parameters such as amount of H_2O_2, catalyst and initial dye concentration on the degradation efficiency were also investigated as follow: The effect of the initial MB concentration on its sonocatalytic degradation was investigated by varying the initial concentration between 5 and 35 mg/L. In this set of experiments, the values of sonocatalyst dosage, the H_2O_2 amount, and the reaction time were set to 25 mg, 1.5 mL, and 140 min, respectively. In order to avoid the use of an excess amount of sonocatalyst, it was essential to determine the optimum value for sonocatalyst dosage in sonocatalytic systems. Therefore, different dosages of the sonocatalyst in the range of 12.5–37.5 mg were tested, while the other parameters such as initial dye concentration, amount of H_2O_2, and reaction time were kept constant at 25 mg/L, 1.5 mL, and 140 min, respectively. The effect of the amount of H_2O_2 on the sonocatalytic degradation was also studied by changing the H_2O_2 amount between 0 and 2 mL. During the experiment, the values of sonocatalyst dosage, initial dye concentration, and reaction time were constant at 25 mg, 25 mg/L, and 140 min, respectively.

In all aqueous solutions containing dye + CdS under ultrasound irradiation, the concentration of Cd in the filtrate after removing the catalyst was less than 0.1%, as confirmed by the ICP-AES analysis of the reaction mixtures.

3. Results and discussion

3.1. Characterization of the sonocatalyst

Among the various methods, the solvothermal method is an important technology for synthesizing inorganic nanostructures at low temperatures. The solvothermal process uses a solvent in the pressure and temperature above its critical point to increase the solubility of a solid as well as speed of reactions [30]. In this paper, the authors report the synthesis of CdS nanoparticles by the hydrothermal decomposition of single-source molecular precursor (Cd(DEDTC)$_2$) in accordance with the following figure (Fig. 1):

Fig. 2 shows the XRD pattern of the product derived from hydrothermal decomposition of the Cd(DEDTC)$_2$ precursor at 200°C for 24 h. It can be seen from Fig. 2 that the prepared product is CdS in both hexagonal and cubic phases (JCPDS Cards no. 75-1545 and 10-0454, respectively). The complex was completely decomposed into CdS and no impurity peaks were found in the XRD pattern. The average size of the CdS particles was found to be approximately 20 nm by the Debye–Scherrer equation [31]: $D_{XRD} = 0.9\lambda/(\beta \cos\theta)$ where D_{XRD} is the average crystalline size, λ is the wavelength of Cu Kα radiation, β is the full width at half maximum of the diffraction peak and θ is the Bragg angle.

Fig. 3 shows FT-IR spectra of Cd(DEDTC)$_2$ complex and its decomposition product. As depicted in Fig. 3(a), complex exhibits two characteristic bands in the range of 1432–1488 and 950–1050 cm^{-1} correspond to the stretching

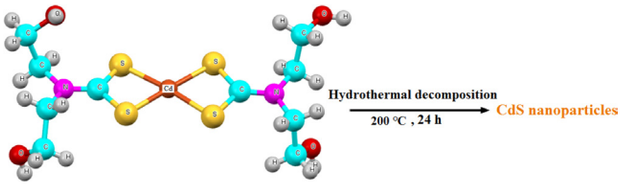

Fig. 1. The preparation of CdS nanoparticles for dyes degradation under ultrasound irradiation.

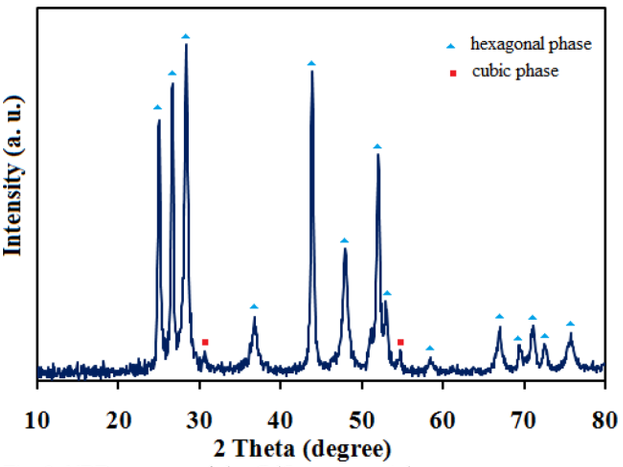

Fig. 2. XRD pattern of the CdS nanoparticles.

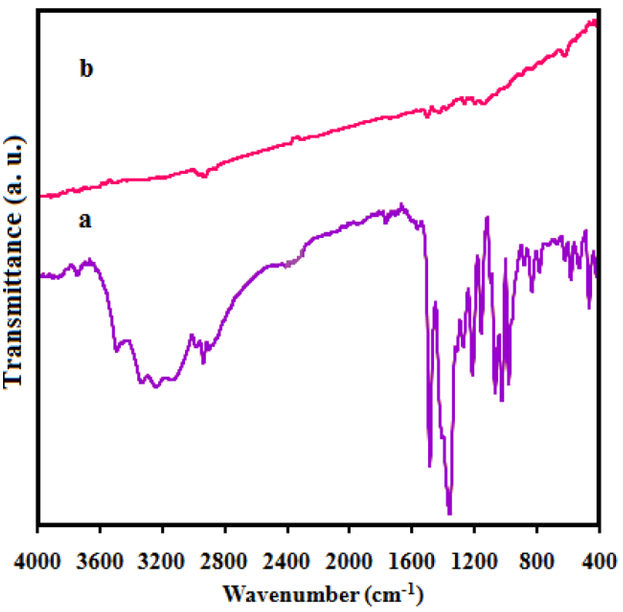

Fig. 3. (a) FT-IR spectra of the Cd(DEDTC)$_2$ complex; (b) CdS nanoparticles.

vibrations of C-N and C-S, respectively [32,33]. As shown in Fig. 3(b), disappearing all the bands of complex after hydrothermal decomposition shows that the complex has been completely decomposed to CdS. It is noted that the Cd-S vibration appears below 400 cm^{-1}.

The morphology and size of the CdS nanoparticles were investigated by SEM. SEM images with different magnification of decomposition product of $Cd(DEDTC)_2$ complex are shown in Fig. 4(a) and (b). As shown in Fig. 4(a) and (b), the product was formed from uniform and fine nanoparticles which loosely aggregated.

Fig. 5 shows TEM images of CdS nanoparticles powder produced by hydrothermal treatment of $Cd(DEDTC)_2$ complex at 200°C. Ultrasonic vibration was employed for dispersing the sample powder in ethanol before TEM. As shown in Fig. 5, the obtained CdS nanoparticles were formed from sphere-like particles. It can be seen that the sizes of CdS nanoparticles are in the range of 10–30 nm. The TEM analysis reveals that the hydrothermal decomposition of $Cd(DEDTC)_2$ complex at 200°C is an appropriate method for the preparation of the CdS nanoparticles with narrow-size distribution.

The chemical purity of the product was also tested by EDX analysis. Fig. 6 shows the EDX spectrum of the synthesized CdS nanoparticles. The spectrum shows that the nanoparticles are mainly composed of cadmium and sulfide. The atomic percentages of Cd and S were found to be 47.25 and 52.75%, respectively for CdS nanoparticles in distilled water. The atomic ratio of Cd and S is about 1:1, which approaches the theoretical value for CdS. This obser-

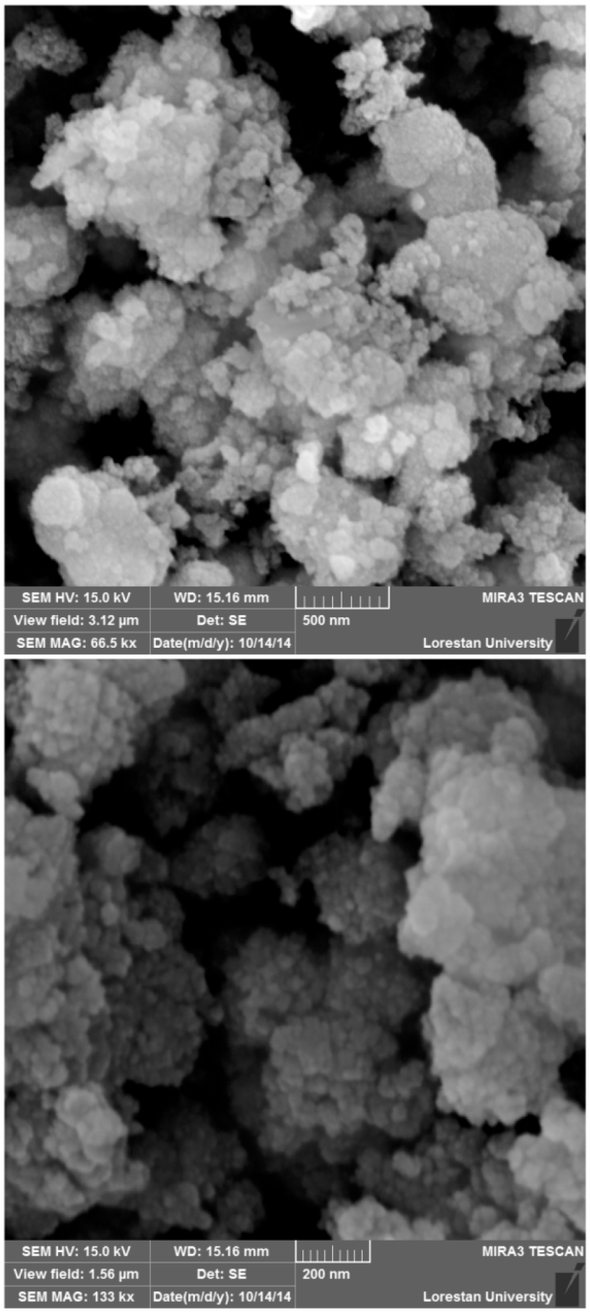

Fig. 4. SEM images of the CdS nanoparticles.

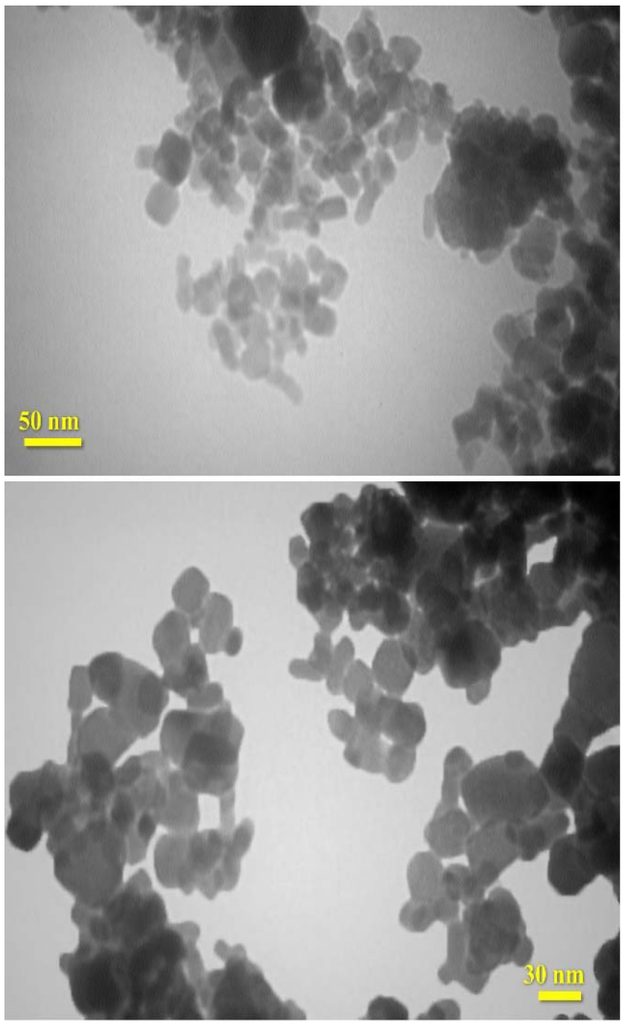

Fig. 5. TEM images of the CdS nanoparticles.

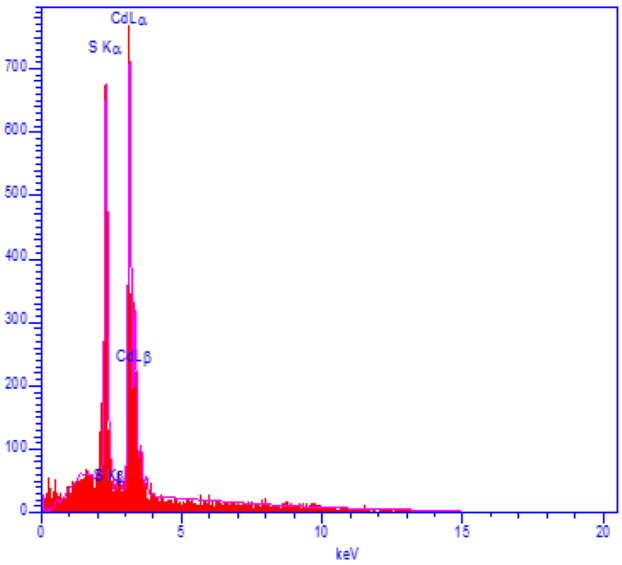

Fig. 6. EDX analysis of the CdS nanoparticles.

vation further confirms that the final product highly pure CdS nanoparticles are.

Fig. 7 shows the absorption spectrum of the sphere-like CdS nanoparticles dispersed in distilled water. This spectrum exhibits defined absorption edge at 488 nm, corresponding to energy gap of 2.3 for the CdS nanoparticles that is similar to the reported values in the literature [34]. This edge is assigned to the optical transition of the first excitonic state. Based on the diagram in Fig. 7, this product could be an appropriate candidate for sonocatalytic purposes.

3.2. Sonocatalytic degradation of dyes

The sonocatalytic activity of the CdS nanoparticles was evaluated by degrading MB under ultrasonic irradiation in the presence of H_2O_2. Fig. 8(a) shows the changes of absorption spectra of 50 mL MB (25 mg/L) at different irradiation times in the system containing CdS nanoparticles (25

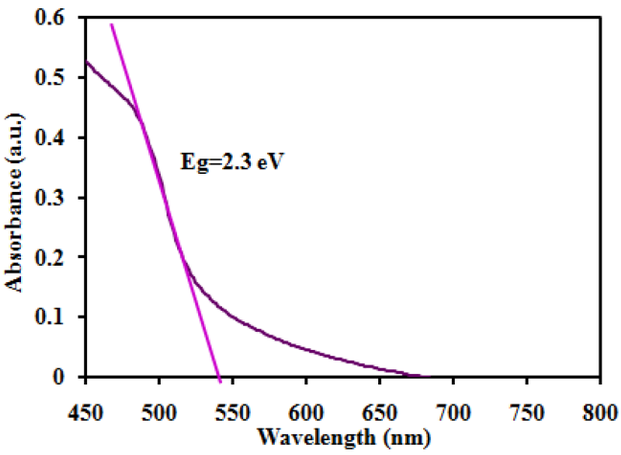

Fig. 7. UV-Vis absorbance spectrum of the CdS nanoparticles.

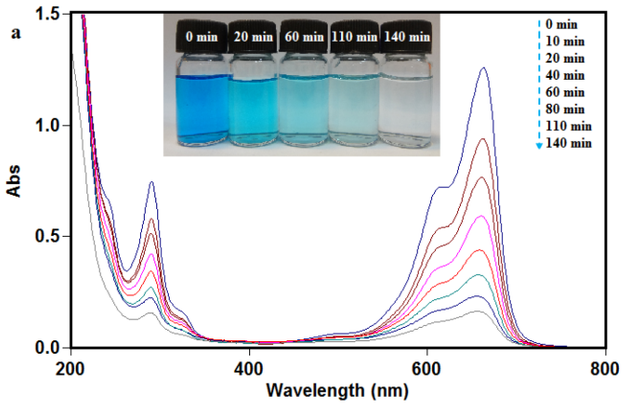

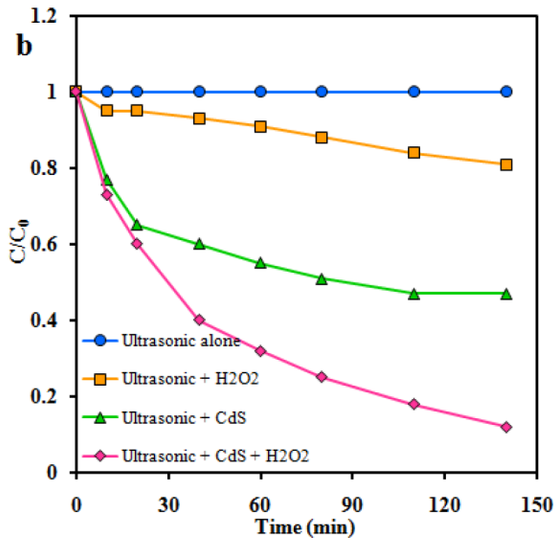

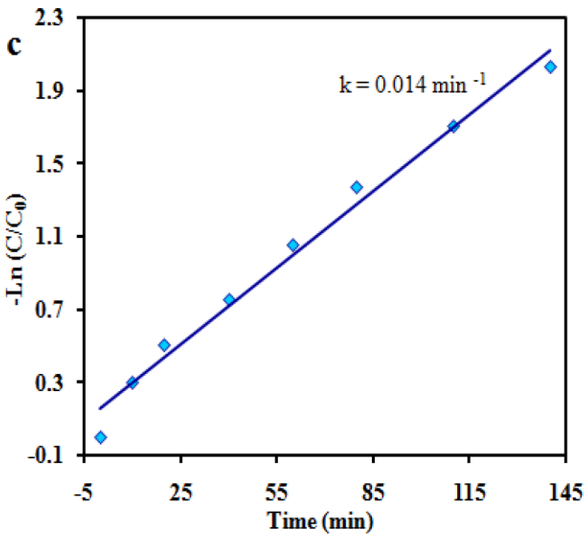

Fig. 8. (a) The absorbance spectra of MB over CdS nanoparticles at different time intervals; (b) concentration changes of MB (C/C_0) at 663 nm as a function of irradiation time; (c) $Ln(C/C_0)$ versus irradiation time in MB solution.

mg) and H_2O_2 (1.5 mL, 1 M). The MB chroma gradually decreased over time (inset in Fig. 8(a)). It can be noted that, the intensity of absorption peak at 663 nm decreased with increasing irradiation time and disappeared after 140 min. Fig. 8(b) displayed the changes in the concentration of MB (C/C_0) at 663 nm as a function of irradiation time for CdS nanoparticles under different conditions. Here, C_0 and C are the dye concentration before and after irradiation, respectively. No appreciable degradation of the MB has been observed under direct sonolysis after 140 min. In the absence of any catalyst, degradation efficiency of MB is lower than 20% after 140 min irradiation. Under ultrasonic irradiation, approximately 52% of MB was removed by CdS nanoparticles without using H_2O_2, probably due to the difficulty of migration of the electron-hole pairs of the CdS nanoparticles. It is worthwhile to note that the sonocatalytic activity was significantly enhanced by adding H_2O_2 to the system of MB and CdS nanoparticles. The sonodegradation rate of MB reached to 87% after ultrasonic irradiation for 140 min, which demonstrated that most of the MB molecules in the solution were degraded. To assess the rate of the photocatalytic degradation of MB, the linearized pseudo-first-order kinetic model was used according to Eq. (2) [35]:

$$-\ln(C/C_0) = k_{app}t \quad (2)$$

where C (mg/L) is the concentration of MB at time t (min). A straight line of $-\ln(C/C_0)$ vs. t indicates the suitability of the model for describing sonocatalytic removal of MB. The slope of the line is the apparent rate constant (k_{app}) as min^{-1}. The result of kinetic study is shown through a smaller figure which is depicted on Fig. 8(c). The obtained correlation coefficient (R = 0.9961) for the pseudo-first-order kinetic model indicated the suitability of the model for predicting the rate of sonocatalytic degradation of MB. Moreover, the slope of the equation (k_{app}) was found to be 0.014 min^{-1}. This indicated the relatively high rate of photocatalytic degradation of MB.

In order to evaluate the scope of this method, the sonocatalytic degradation of other organic dyes such as RhB and MO was investigated under identical conditions. Fig. 9 compares the degradation efficiencies of MB, RhB and MO. The degradation efficiencies of MB, RhB, and MO were 87, 93.17, and 55.27% with rate constants of 0.014 min^{-1}, 0.019 min^{-1}, and 0.004 min^{-1}, respectively. The slow degradation of MO can be related to its high redox potential [36].

3.2.1. Effect of H_2O_2

The influence of H_2O_2 amount on MB degradation over CdS nanoparticles has also been evaluated. The results are shown in Fig. 10. It can be clearly seen that about 52% of MB was degraded without any H_2O_2 within 140 min of reaction. The degradation efficiency of MB was markedly enhanced with adding H_2O_2. When the H_2O_2 amount gradually changed from 0.5 to 1.5 mL, the sonocatalytic degradation rates of MB were greatly improved correspondingly, and about 87% of MB has been decomposed within 140 min of reaction. This enhancement in degradation rate is due to increase in the ·OH radicals with increasing the concentration of H_2O_2. However, a further increase in H_2O_2 content higher than 1.5 mL leads to decrease of the photocatalytic activity. It is well-known that excess H_2O_2 molecules act as

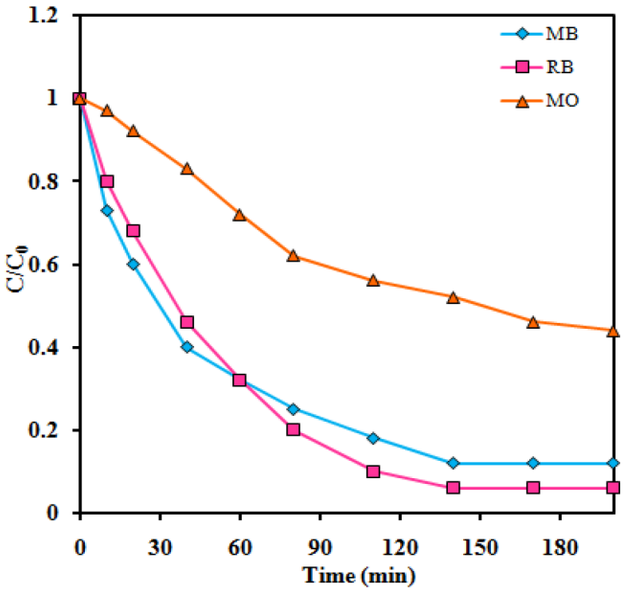

Fig. 9. Comparison of the concentration changes of MB, RB and MO (C/C_0) as a function of irradiation time for CdS nanoparticles. Initial dye concentration: 25 mg/L, the CdS dosage: 25 mg, the amount of H_2O_2: 1M, 1.5 mL and reaction time: 200 min.

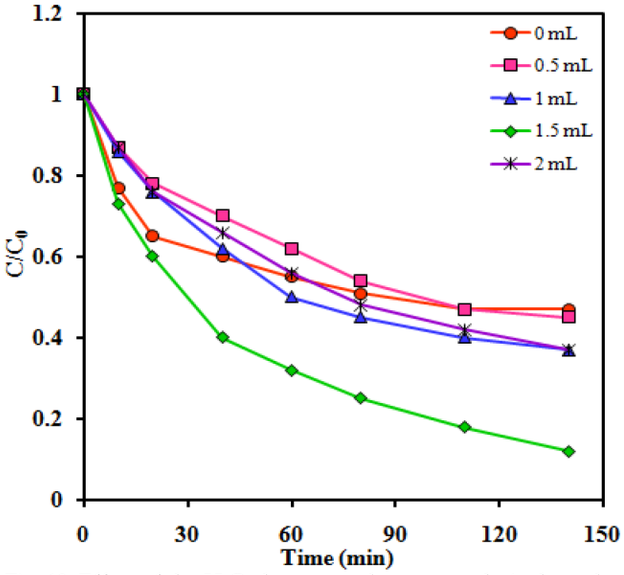

Fig. 10. Effect of the H_2O_2 dosage on the sonocatalytic degradation of MB. Initial dye concentration: 25 mg/L, the CdS dosage: 25 mg and reaction time: 140 min.

scavenger of ·OH radicals to generate perhydroxyl (HOO·) radicals with lower oxidation potential (Eq. (3)) [37,38].

$$H_2O_2 + \cdot OH \rightarrow H_2O + HOO\cdot \quad (3)$$

3.2.2. Effect of catalyst dosage

The data of examined effect of the catalyst dosage on sonocatalytic MB degradation are shown in Fig. 11. The

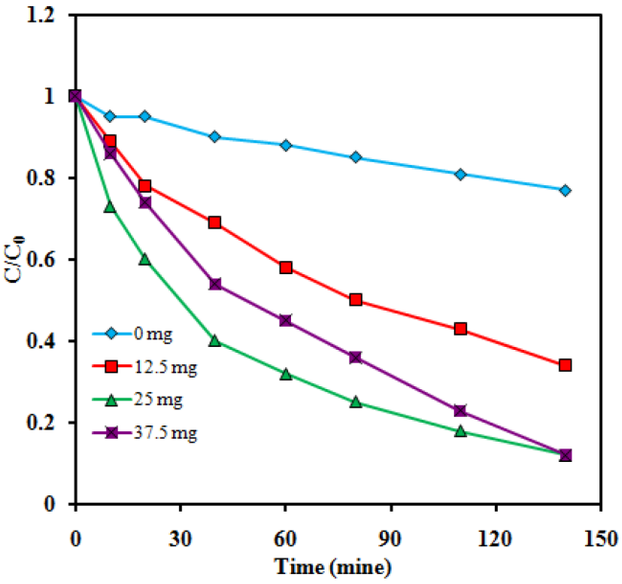

Fig. 11. Effect of the CdS dosage on the sonocatalytic degradation of MB. Initial dye concentration: 25 mg/L, the amount of H_2O_2:1M, 1.5 mL and reaction time: 140 min.

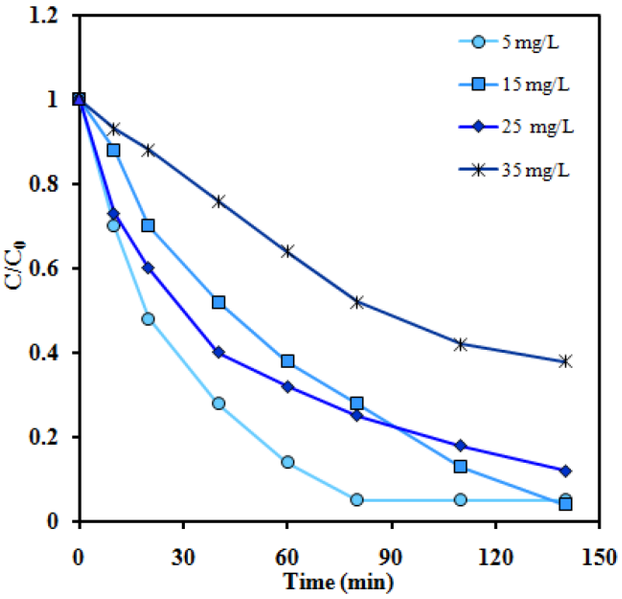

Fig. 12. Sonocatalytic degradation efficiency for different initial dye concentrations. The CdS dosage: 25 mg, the amount of H_2O_2: 1M, 1.5 mL and reaction time: 140 min.

degradation efficiency of MB is lower than 20% after 140 min of continuous reaction in the absence of the CdS nanoparticles.With increasing CdS dosage to 12.5 mg, the sonocatalytic degradation of MB was found to be 65% for 140 min. The MB degradation efficiency increased to 87% with increasing dosage of the CdS nanoparticles to 25 mg. The addition of more CdS nanoparticles into the solution provides more active reaction sites for the generation of •OH radicals, accelerating the degradation rate. Moreover, increasing the sonocatalyst dosage creates the additional nuclei for the cavitation phenomenon and generating more •OH radicals [39]. However, increasing CdS nanoparticles dosage from 25 to 37.5 mg, dose not lead to increase the degradation efficiency. In fact, the aggregation of sonocatalyst particles occurs in the solution at higher dosages. This leads to the loss of effective surface area and surficial active sites for the generation of •OH radicals. Furthermore, the extent of cavitation phenomenon is depended on the active surface area of the applied sonocatalyst. So, in the presence of excess amount of the sonocatalyst, lower amount of ultrasonic waves could be passed into the solution to create cavitation bubbles [40,41].

3.2.3. Effect of initial dye concentration

The effect of the initial MB concentration was investigated by varying the initial MB concentrations between 5 and 35 mg/L (Fig. 12). The MB degradation efficiency decreased from 94% to 62% with increasing initial MB concentration from 5 to 35 mg/L within a reaction time of 140 min. This indicated the need for more time to achieve the appropriate removal efficiency of MB at higher concentrations. Similarly, Song et al. have reported approximately same trend based on their study on the sonocatalysis of various organic dyes [42]. Clearly, the number of ·OH needed for sonocatalysis of MB increases with increasing its initial concentration, resulting in lower efficiency of the process. Decreasing degradation efficiency with increasing initial concentration may be due to the limited number of active sites for the subsequent generation of hydroxyl radicals to degrade high initial concentrations at specified reaction time [43,44].

3.2.4. Proposed mechanism for sonocatalytic degradation of dyes

It is well-known that the sonocatalytic degradation of organic pollutants over a sonocatalyst is based upon three theories including sonoluminescence, "hot spot" and oxygen atom escape [45–47]. Sonoluminescence can occur when a sound wave has the sufficient intensity and induces quickly collapsing gaseous cavities within a liquid. These cavities may be generated through a process known as "cavitations" or form pre-existing bubbles. Sonoluminescence can be made to be stable in the laboratory, and then a single bubble will periodically expand and collapse over and over again emitting a burst of light each time it collapses. Therefore, ultrasonic irradiation conduce sonoluminescence phenomenon leading to produce a lot of light. It has been well known that the generated light has a relatively wide range of wavelengths because of acoustic cavitations. The produced light with wavelengths below 375 nm can undoubtedly excite the CdS particles result in acting as a sonocatalyst.

Based on the above results, a possible sonocatalytic mechanism over CdS nanoparticles has been proposed as follows and illustrated in Fig. 13 [48–50]. Under light irradiation generated by sonoluminescence phenomena, the electrons are excited from valence band (VB) of CdS to conduction band (CB) and the electron–hole pairs are formed in the inner or on the surface of CdS nanoparticles (Eq. (4)).

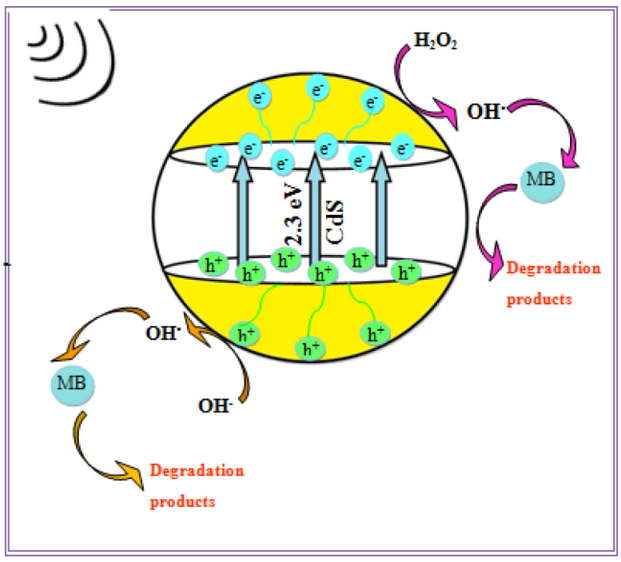

Fig. 13. Schematic drawing of separation of generated electrons and holes on the interface of CdS nanoparticles under ultrasonic irradiation.

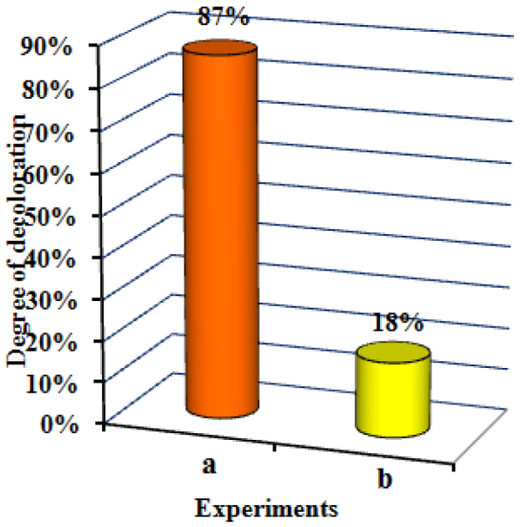

Fig. 14. Sonodegradation of MB over CdS nanoparticles: (a) alone, (b) in the presence of 20 mM t-BuOH. The CdS dosage: 25 mg, initial MB concentration: 25 mg/L, the amount of H_2O_2: 1M, 1.5 mL and reaction time: 140 min.

The generated electrons react with dissolved H_2O_2 in aqueous solution and produce the hydroxyl radicals (·OH) through a series of chemical reactions, which degrade the organic pollutants in the solution (Eq. (5)). At the same time, the generated holes oxidize H_2O or OH^- species (from H_2O_2) on the surface of CdS nanoparticles to produce the hydroxyl radicals (·OH) (Eq. (6)). These hydroxyl radicals (·OH) with high oxidizing activity degrade the organic dye to CO_2, H_2O and other products (Eq. (7)).

$$\mathrm{CdS} + \mathrm{ultrasound} \rightarrow e^-_{CB} + h^+_{VB} \quad (4)$$

$$e^-_{CB} + H_2O_2 \rightarrow OH^- + OH\cdot \quad (5)$$

$$h^+_{VB} + \frac{OH^-}{(H2O)} \rightarrow OH\cdot \quad (6)$$

$$\mathrm{dye} + OH\cdot \rightarrow \mathrm{degradation\ products}\,(CO_2, H_2O, \mathrm{etc}) \quad (7)$$

To confirm the above-suggested mechanism, *t*-butyl alcohol (*t*-BuOH) was added to the reaction mixture as a scavenger to determine the reactive ·OH species. As shown in Fig. 14, the sonocatalytic degradation of MB was significantly decreased by adding *t*-BuOH to the reaction mixture. This finding confirms that the ·OH radicals are the main active oxidizing species in the degradation process [51].

3.2.5. Reusability test

In order to establish the reusability and stability of the CdS nanoparticles sonocatalyst, it was separated from the reaction mixture after its first use for degradation of MB. The recovered catalyst was found to be reusable for four runs without significant loss in activity (Fig. 15(a)). At the same time, the concentration of Cd in the filtrate was determined to be less than 0.1 % by ICP-AES. We have also tested the nature of the recovered catalyst. As shown in Fig. 15(b) and (c), the XRD and FT-IR spectra of the recovered CdS did not show significant changes after the fourth run compared to the fresh catalyst (see Figs. 2 and 3). These observations confirm that the structure of the CdS nanoparticles was stable under the reaction conditions and was not affected by the reactants.

4. Conclusions

In this study, CdS nanoparticles were successfully produced by a facile hydrothermal reaction and their sonocatalytic performance was evaluated by degrading organic dyes under ultrasonic irradiation in the presence of H_2O_2 as a hydroxyl radical (·OH) source. The XRD analysis showed crystallized nature of CdS with both hexagonal and cubic phases. In addition, the experimental results also demonstrated the feasibilities of the sonocatalytic degradation of MB and other organic pollutants for wastewater treatment. The sonocatalytic degradation of MB is proven to be depended on the initial concentrations of MB, amount of CdS nanoparticles, and amount of H_2O_2. This study provides a green, low-cost, simple and rapid procedure for the degradation of organic dyes pollutants in aqueous wastewater solutions.

Acknowledgments

The authors thankfully appreciate the Lorestan University and Iran Nanotechnology Initiative Council (INIC) for their financial supports.

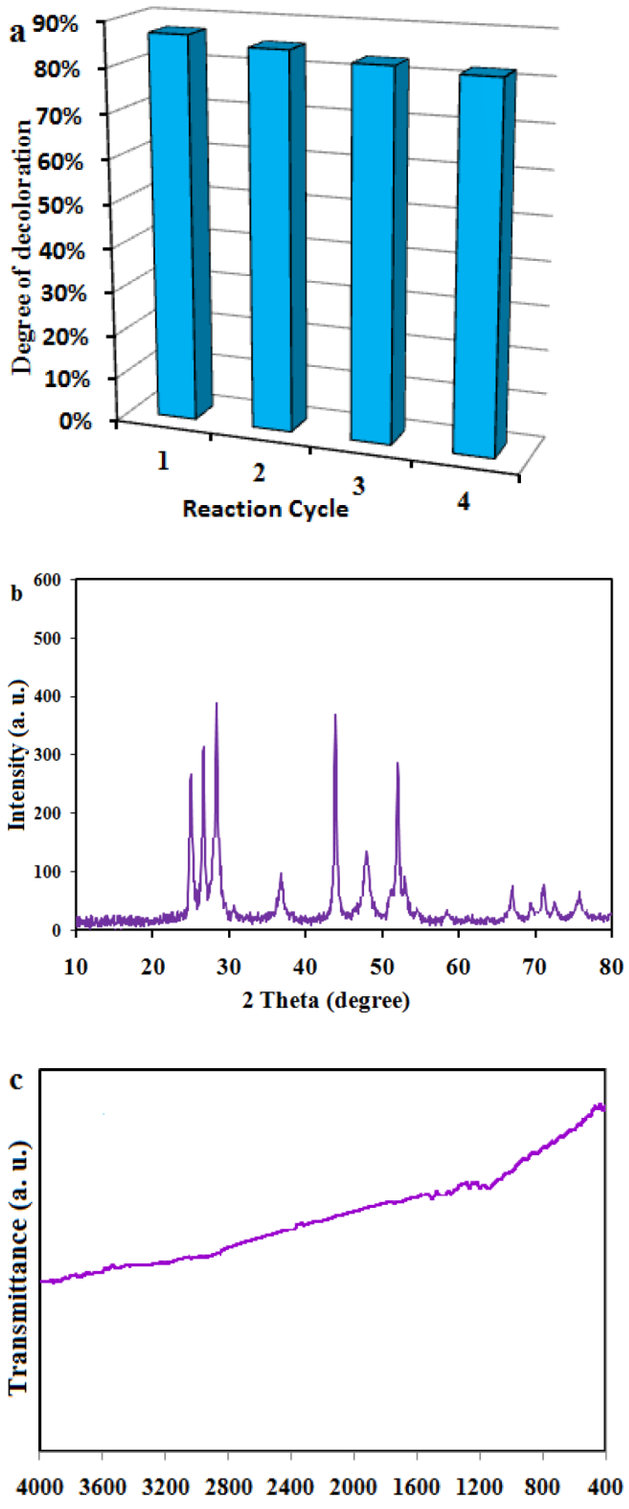

Fig. 15. (a) Recyclability of CdS nanoparticles, (b) XRD and (c) FT-IR of the recovered CdS nanopaticles after the fourth run.

References

[1] M.A. Al-Ghouti, M.A.M. Khraisheh, S.J. Allen, M N. Ahmad, The removal of dyes from textile wastewater: a study of the physical characteristics and adsorption mechanisms of diatomaceous earth, J. Environ. Manage., 69 (2003) 229–238.

[2] M.W. Xiao, L.S. Wang, Y.D. Wu, X.J. Huang, D. Zhi, Preparation and characterization of CdS nanoparticles decorated into titanate nanotubes and their photocatalytic properties, Nanotechnology, 19 (2008) 015706–015712.

[3] J.K. Zhou, L. Lv, J. Yu, H.L. Li, P.Z. Guo, H. Sun, X.S. Zhao, Synthesis of self-organized polycrystalline F-doped TiO_2 hollow microspheres and their photocatalytic activity under visible light, J. Phys. Chem., C 112 (2008) 5316–5321.

[4] R.D.C. Soltani, A. Rezaee, A. Khataee, Combination of carbon black–ZnO/UV process with an electrochemical process equipped with a carbon black–PTFE-coated gas-diffusion cathode for removal of a textile dye, Ind. Eng. Chem. Res., 52 (2013) 14133–14142.

[5] R.D.C. Soltani, A. Rezaee, A.R. Khataee, M. Safari, Photocatalytic process by immobilized carbon black/ZnO nanocomposite for dye removal from aqueous medium: optimization by response surface methodology, J. Ind. Eng. Chem., 20 (2014) 1861–1868.

[6] A. Khataee, M. Fathinia, Y. Hanifehpour, S.W. Joo, Kinetics and mechanism of enhanced photocatalytic activity under visible light using synthesized $Pr_xCd_{1-x}Se$ nanoparticles, Ind. Eng. Chem. Res., 52 (2013) 13357–13369.

[7] F. He, J. Fan, D. Ma, L.M. Zhang, C. Leung, H.L. Chan, The attachment of Fe_3O_4 nanoparticles to graphene oxide by covalent bonding, Carbon, 48 (2010) 3139–3144.

[8] S. Qadri, A. Ganoe, Y. Haik, Removal and recovery of acridine orange from solutions by use of magnetic nanoparticles, J. Hazard. Mater., 169 (2009) 318–323.

[9] Z.G. Feng, Y. Lin, X.X. Yu, Q.H. Shen, L. Ma, Z.Y. Li, N. Pan, X.P. Wang, Highly efficient dye adsorption and removal: a functional hybrid of reduced grapheme oxide–Fe_3O_4 nanoparticles as an easily regenerative adsorbent, J. Mater. Chem., 22 (2012) 3527–3535.

[10] M. Rafatullaha, O. Sulaimana, R. Hashima, A. Ahmad, Adsorption of methylene blue on low-cost adsorbents: A review, J. Hazard. Mater., 177 (2010) 70–80.

[11] N. Ertugay, F.N. Acar, Decolorization of Direct Blue 71 using UV irradiation and ultrasound in the presence of TiO_2 catalyst, Desalin. Water. Treat., 57 (2015) 9318–9324.

[12] H. Jiang, J. Li, Z. Mu, H. Geng, Degradation of methyl orange through synergistic effect of Cu/Cu_2O nanoporous composite and ultrasonic wave, Desal. Water. Treat., 56 (2014) 173–180.

[13] A. Khataee, A. Karimi, S. Arefi-Oskoui, R.D.C. Soltani, Y. Hanifehpour, B. Soltani, S.W. Joo, Sonochemical synthesis of Pr-doped ZnO nanoparticles for sonocatalytic degradation of Acid Red 17, Ultrason. Sonochem., 22 (2014) 371–381.

[14] G. Li, W. Zhao, B. Wang, Q. Gu, X. Zhang, Synergetic degradation of Acid Orange 7 by fly ash under ultrasonic irradiation, Desal. Water. Treat., 57 (2014) 2167–2174.

[15] G. Li, Y. Feng, B. Wang, M. Wang, Contribution of hydroxyl radicals to the degradation of Acid Orange 7 by fly ash under ultrasonic irradiation, Desal. Water. Treat., 57 (2015) 18168–18174.

[16] P. Singh, M.C. Vishnu, K.K. Sharma, R. Singh, S. Madhav, D. Tiwary, P.K. Mishra, Comparative study of dye degradation using TiO_2-activated carbon nanocomposites as catalysts in photocatalytic, sonocatalytic, and photosonocatalytic reactor, Desal. Water. Treat., 57(43) (2016) 20552–20564.

[17] Z.D. Meng, W.C. Oh, Sonocatalytic degradation and catalytic activities for MB solution of Fe treated fullerene/TiO_2 composite with different ultrasonic intensity, Ultrason. Sonochem., 18 (2011) 757–764.

[18] S. Zhang, Synergistic effects of C–Cr codoping in TiO_2 and enhanced sonocatalytic activity under ultrasonic irradiation, Ultrason. Sonochem., 19 (2012) 767–771.

[19] Y. Wang, L. Gai, W. Ma, H. Jiang, X. Peng, L. Zhao, Ultrasound-assisted catalytic degradation of methyl orange with Fe_3O_4/polyaniline in near neutral solution, Ind, Eng. Chem. Res., 54 (2015) 2279–2289.

[20] N. Wang, L. Zhu, M. Wang, D. Wang, H. Tang, Sono-enhanced degradation of dye pollutants with the use of H_2O_2 activated by Fe_3O_4 magnetic nanoparticles as peroxidase mimetic, Ultrason. Sonochem., 17 (2010) 78–83.
[21] A.R. Khataee, R.D.C. Soltani, A. Karimi. S.W. Joo, Sonocatalytic degradation of a textile dye over Gd-doped ZnO nanoparticles synthesized through sonochemical process, Ultrason. Sonochem., 23 (2015) 219–230.
[22] R.D.C. Soltani, M. Safari, M. Mashayekhi, Sonocatalyzed decolorization of synthetic textile wastewater using sonochemically synthesized MgO nanostructures, Ultrason. Sonochem., 30 (2016) 123–131.
[23] J. Wang, Z. Jiang, L. Zhang, P. Kang, Y. Xie, Y. Lv, R. Xu, X. Zhang, Sonocatalytic degradation of some dyestuffs and comparison of catalytic activities of nano-sized TiO_2, nano-sized ZnO and composite TiO_2/ZnO powders under ultrasonic irradiation, Ultrason. Sonochem., 16 (2009) 225–231.
[24] X. Liu, L. Pan, T. Lv, G. Zhu, Z. Sun, C. Sun, Microwave-assisted synthesis of CdS-reduced graphene oxide composites for photocatalytic reduction of Cr(vi), Chem. Commun., 47 (2010) 11984–11986.
[25] K. Keis, E. Magnusson, H. Lindstrom, S.E. Lindquist, A. Hagfeldt, A 5% efficient photo electrochemical solar cell based on nanostructured ZnO electrodes, Sol. Energy Mater. Sol. Cells., 73 (2002) 51–58.
[26] B. Kaboudin, F. Kazemi, A. Ghaderian, Z. Zand, A novel and simple method for the preparation of hexagonal CdS nanoparticles: synthesis, characterization, and uses in photocatalytic reduction of nitrobenzenes to aminobenzenes using sunlight. J. Iran. Chen Soc., 11 (2014) 1121–1127.
[27] Q. Xiang, B. Cheng, J. Yu, Hierarchical porous CdS nanosheet-assembled flowers with enhanced visible-light photocatalytic H_2-production performance. Appl. Catal. B. Environ., 138–139 (2013) 299–303.
[28] L. Zhang, Z. Cheng, D. Wang, J. Li, Preparation of popcorn-shaped CdS nanoparticles by hydrothermal method and their potent photocatalytic degradation efficiency. Mater. Lett., 158 (2015) 439–441.
[29] B. Ahmed, S. Kumar, A.K. Ojha, Shape induced (spherical, sheets and rods) optical and magnetic properties of CdS nanostructures with enhanced photocatalytic activity for photodegradation of methylene blue dye under ultra-violet irradiation. J. Alloys Comp., 679 (2016) 324–334.
[30] K.B. Tang, Y.T. Qian, J.H. Zeng, X.G. Yang, Solvothermal route to semiconductor nanowires, Adv. Mater., 15 (2003) 448–450.
[31] H.P. Klug, L.E. Alexander, X-Ray Diffraction Procedures: For Polycrystalline and Amorphous Materials, 2nd ed., Wiley, New York. 1974.
[32] X.Y. Chen, Z.H. Wang, X. Wang, J.X. Wan, J.W. Liu, Y. Qian, Single source approach to cubic FeS_2 crystallites and their optical and electrochemical properties, Inorg. Chem., 44 (2005) 951–954.
[33] K. Ariga, A. Vinu, M. Miyahara, Recent progresses in bio-inorganic nanohybrids, Curr. Nanosci., 2 (2006) 197–210.
[34] M.F. Kotkata, A.E. Masoud, M.B. Mohamed, E.A. Mahmoud, Synthesis and structural characterization of CdS nanoparticles, Physica. E., 41 (2009) 1457–1465.
[35] H. Zhang, C. Wei, Y. Huang, J. Wang, Preparation of cube micrometer potassium niobate ($KNbO_3$) by hydrothermal method and sonocatalytic degradation of organic dye, Ultrason. Sonochem., 30 (2016) 61–69.
[36] S.B. Khan, M. Faisal, M.M. Rahman, A. Jamal, Exploration of CeO_2 nanoparticles as a chemi-sensor and photo-catalyst for environmental applications, Sci. Total Environ., 409 (2011) 2987–2992.
[37] L. Ai, C. Zhang, L. Li, J. Jiang, Iron terephthalate metal–organic framework: Revealing the effective activation of hydrogen peroxide for the degradation of organic dye under visible light irradiation, Appl. Catal. B. Environ., 148–149 (2014) 191–200.
[38] A.R. Khataee, P. Gholami, B. Vahid, S.W. Joo, Heterogeneous sono-Fenton process using pyrite nanorods prepared by non-thermal plasma for degradation of an anthraquinone dye, Ultrason. Sonochem., 32 (2016) 357–370.
[39] N. Ertugay, F.N. Scar, The degradation of Direct Blue 71 by sono, photo and sonophotocatalytic oxidation in the presence of ZnO nanocatalyst, Appl. Surf. Sci., 318 (2014) 121–126.
[40] J. Bandara, J. Mielczarski. J. Kiwi, Molecular mechanism of surface recognition. Azo dyes degradation on Fe, Ti, and Al oxides through metal sulfonate complexes, Langmuir., 15 (1999) 7670–7679.
[41] J. Wu, H. Zhang, J. Qiu, Degradation of Acid Orange 7 in aqueous solution by a novel electro/Fe^{2+}peroxydisulfate process, J. Hazard. Mater., 215 (2012) 138–145.
[42] L. Song, S. Zhang, X. Wu, Q. Wei, A metal-free and graphitic carbon nitride sonocatalyst with high sonocatalytic activity for degradation methylene blue, Chem. Eng. J., 184 (2012) 256–260.
[43] J. Wang, Z. Pan, Z. Zhang, X. Zhang, F. Wen, T. Ma, Y. Jiang, L. Wang, L. Xu, P. Kang, Sonocatalytic degradation of methyl parathion in the presence of nanometer and ordinary anatase titanium dioxide catalysts and comparison of their sonocatalytic abilities, Ultrason. Sonochem., 13 (2006) 493–500.
[44] R.D.C. Soltani, A.R. Khataee, M. Mashayekhi, Photocatalytic degradation of a textile dye in aqueous phase over ZnO nanoparticles embedded in biosilica nanobiostructure, Desal. Water Treat., 57 (2016) 13494–13504.
[45] Y. Segura, R. Molina, F. Martnez, J.A. Melero, Integrated heterogeneous sono-photo Fenton processes for the degradation of phenolic aqueous solutions, Ultrason. Sonochem., 16 (2009) 417–424.
[46] M.H. Entezari, Z. Sharif Al-Hoseini, Sono-sorption as a new method for the removal of methylene blue from aqueous solution, Ultrason. Sonochem., 14 (2007) 599–604.
[47] J. Saien, H. Delavari, A.R. Solymani, Sono-assisted photocatalytic degradation of styrene-acrylic acid copolymer in aqueous media with nanotitania particles and kinetic studies, J. Hazard. Mater., 177 (2010) 1031–1038.
[48] X.W. Zhang, M.H. Zhou, L.C. Lei, Preparation of photocatalytic TiO_2 coating of nanosized particles supported on activated carbon by AP-MOCVD, Carbon, 43 (2005) 1700–1708.
[49] F.J. Zhang, M.L. Chen, K. Zhang, W.C. Oh, Visible light photoelectrocatalytic properties of novel yttrium treated carbon nanotube/titania composite electrodes Bull. Korean Chem. Soc., 31 (2010) 133–138.
[50] J. Wang, Y.W. Guo, B. Liu, X.D. Jin, L.J. Liu, R. Xu, Y.M. Kong, B.X. Wang, Detection and analysis of reactive oxygen species (ROS) generated by nanosized TiO_2 powder under ultrasonic irradiation and application in sonocatalytic degradation of organic dyes, Ultrason. Sonochem., 18 (2011) 177–183.
[51] F. Soumia, C. Petrier, Effect of potassium monopersulfate (oxone) and operating parameters on sonochemical degradation of cationic dye in an aqueous solution, Ultrason. Sonochem., 32 (2016) 343–347.